Thermodynamic performance assessment of carbon dioxide blends with low-global warming potential (GWP) working fluids for a heat pump water heater☆

Baomin Dai[a], Chaobin Dang[b], Minxia Li[*a], Hua Tian[c], Yitai Ma[a]

[a] *Key Laboratory of Efficient Utilization of Low and Medium Grade Energy, MOE, Tianjin University, Tianjin 300072, China*
[b] *Department of Human and Engineered Environmental Studies, The University of Tokyo, Chiba 277-8563 Japan*
[c] *State Key Laboratory of Engines, Tianjin University, Tianjin 300072, China*

[*]Corresponding author. Tel.: +86 022 27406040; fax: +86 022 27404741.

E-mail address: tjmxli@tju.edu.cn (M. Li); dbm@tju.edu.cn (B. Dai)

Abstract: Blends of CO_2 with ten low-global warming potential (GWP) working fluids are evaluated for use in a heat pump water heater. The effects that the discharge pressure, component ratio (X_{CO2}), hot-water outlet temperature and chilled water inlet temperature have on the coefficient of performance (COP) of heat pump are analyzed when the pinch point of the heat exchange is considered . It is found that the temperature glide of zeotropic mixture has a good thermal match with the temperature change of water as two pinch points appear in the gas cooler/condenser . The good thermal match in the heat exchanger promotes COP of heat pump. Addition of low-GWP working fluids to pure CO_2 can reduce high-side pressure. The results show that CO_2/R41 and CO_2/R32 are suitable candidates for heat pump water heaters because of their high COP and low high-side pressure in comparison with those of a pure CO_2 cycle.

Keywords: CO_2; low-GWP refrigerant; zeotropic; heat pump water heater; pinch point; thermal match

☆The original paper was presented on the 11th IIR Gustav Lorentzen Conference on Natural Refrigerants (GL2014), Aug. 31 to Sept. 2, 2014, Hangzhou, China.

Nomenclature

E	exergy (kJ/kg)
h	specific enthalpy (kJ/kg)
I	irreversibility (kJ/kg)
m	mass flow rate (kg/s)
s	specified entropy (kJ/(kg K))
T	temperature (°C)
P	pressure (MPa)
Q	heat exchange capacity (kW)
W	power input (kW)
X_{CO2}	mass fraction of CO_2 (-)
Subscripts	
0	dead state
1, 2, 2s, 3, 4	state point
b	boiling
C	gas cooler/condenser
Carnot	Carnot
CW	chilled water
Com	compressor
Cri	critical
E	evaporator
e	electrical
Exe	exergy
Exp	expansion valve
HW	hot water
In	inlet
m	mechanical
Opt	optimal
Pinch	pinch point
r	refrigeration
Tot	total
TP	thermodynamic perfectibility
W	water
Greek symbols	
η	efficiency
Acronyms	
COP	coefficient of performance
CP	critical point
GWP	global warming potential
HC	hydrocarbon
HCFC	hydrochlorofluorocarbon
HFC	hydrofluorocarbon
HFO	hydrofluoroolefin
HVAC&R	heating, ventilation, air-conditioning and refrigeration
LEL	lower explosive limit
MAC	mobile air-conditioning
ODP	ozone depletion potential
OEL	occupational exposure limit
PP	pinch point

1. Introduction

The working fluid selection for an air-conditioning and refrigeration system is not only determined by thermodynamic properties, but is also largely related to environmental constraints. The use of chlorinated substances, such as chlorofluorocarbons (CFCs) and hydrochlorofluorocarbons (HCFCs), has been successfully reduced by the Montreal Protocol (UNEP, 1987). The Kyoto Protocol (UNFCCC, 1997) depicted the reduction of the emission of refrigerants with high global warming potentials (GWPs). The European Union fluorinated greenhouse gases (F-gas) regulation (Regulation (EU) No 517/2014) demands a phase-out of the use of F-gas with GWP above 150 in domestic refrigerators and freezers by January 1, 2015, and in new types of mobile air-conditioning (MAC) systems by January 1, 2017. In order to respect the environmental issues and follow the new proposed regulations, great effort has been made to identify the next generation of candidate refrigerants. Consequently, several approaches are under consideration, including low-GWP refrigerants, natural refrigerants, and refrigerant mixtures (Miyara et al., 2012).

Among the low-GWP refrigerants, new synthetic refrigerants hydrofluoroolefins (HFOs) such as R1234yf and R1234ze, which have zero ozone depletion potential (ODP) and a low GWP of 1, are getting increasing attention as alternatives to R134a. However, these two HFOs have more complex molecule structures than most HFCs, and will be more costly (McLinden et al., 2014). Moreover, they are classified as "A2L" in the ASHRAE standard 34 safety group (ANSI/ASHRAE Standard 34-2010), because of their mild flammability. In addition, because of their relatively low operation pressure, the pressure drops that occur in the pipelines and the heat exchanger have a significant influence on system performance. Apart from the HFOs, several HFCs (R152a, R161, and R41) and hydrocarbons (R290, R1270, R600, R600a, R601, and R601a) that have a GWP below 150 are also promising candidates for HVAC&R applications. Nevertheless, some of them possess moderate flammability or require a high operating pressure.

In the class of natural refrigerants including CO_2, NH_3, and HCs, CO_2 is considered to be the most promising refrigerant because of its advantages in practical applications (Lorentzen, 1994, 1995; Lorentzen and Pettersen, 1993), such as zero ODP, GWP of 1, non-toxicity, non-flammability, easy availability, compatibility with lubricants, and excellent thermophysical and transport properties. CO_2 can be used in various refrigeration, air-conditioning, and heat pump systems, especially domestic water heating systems (Kim et al., 2004). A domestic CO_2 heat pump water heater was first commercialized in 2001, and by 2008 the system had shipped over 500,000 units (Miyara et al., 2012). However, the following two main factors restrict the widespread use of the CO_2 system:

- The system operates at a significantly high pressure, which leads to higher initial cost because of the requirement of high-pressure bearings. Moreover, the safety during operation should also be carefully considered.
- Large throttling losses and irreversibility occur during the expansion process, which decrease the whole system performance.

In order to reduce the high-side pressure and improve the energy efficiency of a CO_2 system, some researchers proposed the use of zeotropic refrigerant mixtures of CO_2 and eco-friendly refrigerants. The previous studies are listed as follows:

Kim and Kim (2002) investigated the performance of zeotropic mixtures of CO_2/R134a and CO_2/R290 used in an autocascade refrigeration system. Both simulation and experimental studies were carried out, and the results indicate that as the CO_2 concentration decreases, the COP tends to increase while the high-side pressure declines. Di Nicola et al. (2005) analyzed blends of CO_2 with several HFCs (including R125, R41, R32, and R23) for a low-temperature-stage working fluid used in a cascade refrigeration cycle. They concluded that the CO_2 blends are preferable for cascade systems with a low-temperature approaching 200 K. They also studied the characteristics of blends of CO_2 with natural refrigerants (R170, R290, R1150, R1270, and RE170) used in a cascade refrigeration cycle (Di Nicola et al., 2011). Kim et al. (2008) studied blends of CO_2/R290 and indicated that the discharge pressure of the mixtures decreases with an increase of the R290 fraction. Furthermore, adding R290 to CO_2 improves the system energy efficiency, but reduces the cooling capacity. They also indicated the importance of appropriate temperature matching of the zeotropic refrigerant mixture with the heat transfer fluid, in order to improve the refrigeration system efficiency. Sarkar and Bhattacharyya (2009) proposed blends of CO_2/R600 and CO_2/R600a as working fluids for medium- and high-temperature heating applications. Simulation results showed that the blends could be employed in heat pumps for simultaneous cooling and heating applications, with effective performance. The CO_2/R600a blend is recommended as the best alternative refrigerant to R114 for a high-temperate heat pump, because of its superior COP and lower high-side pressure in comparison with CO_2 systems. Niu and Zhang (2007) tested a binary mixture of CO_2/R290 (71/29 mole fraction) for a cascade refrigeration cycle. The results revealed that the COP and cooling capacity of the mixture are both higher than those of R13, especially

when the evaporation temperature is above 201 K. Onaka et al. (2010) analyzed the heat pump performance using a zeotropic mixture of CO_2/RE170 for a hot water supply system, with the CO_2 mass concentration ranging from 0 to 1. They concluded that the system obtains a maximum COP at a certain heat-rejection pressure for each mixture, and the COPs of the mixtures and the pure RE170 are higher than that of pure CO_2. The irreversibility of each component of the system was also discussed. Zhang et al. (2013) theoretically and experimentally investigated a transcritical cycle operating with CO_2/R290 with a CO_2 mass fraction larger than 0.78. They proposed a correlation for the prediction of optimal heat rejection pressure and verified the simulation results with experimental data. Hakkaki-Fard et al. (2014) developed a numerical model to simulate refrigerant mixtures used for a cold-climate air-source heat pump. They concluded that the heat pump using the mixture of CO_2/R32 (20/80) shows the best improvement in heating capacity. Dai et al. (2014) also studied blends of CO_2 with low-GWP working fluids used in a transcritical Rankine cycle for low-grade heat recovery. The binary mixtures show better thermodynamic performance than the pure CO_2. As can be seen from the above studies, the addition of low-GWP refrigerants to CO_2 can improve the energy performance and reduce the high-side pressure of a CO_2 heat pump/refrigeration system. Moreover, the flammability of the added component, such as HFCs and HCs, can be reduced because of the dilution effect of pure CO_2 (Chen et al., 2009; Kondo et al., 2006).

Yang et al. (2005) performed an exergy analysis of the transcritical carbon dioxide refrigeration cycles with a throttling valve and with an expander, and concluded that the main exergy losses occur in the gas cooler and the compressor. Then, a further study (Yang et al., 2007) compared three different variations of transcritical carbon dioxide two-stage compression cycles with expanders, and the exergy efficiencies were achieved. Tao et al. (2010) experimentally and theoretically analyzed a CO_2 residential air-conditioning with an internal heat exchanger. They concluded that the exergy loss in the gas cooler is the highest one, accounting about 30.7% of the total exergy loss in the system. Sun and Ma (2011) investigated the exergy loss in a transcritical carbon dioxide refrigeration cycle with ejector and with throttling valve. They found that ejector instead of throttling valve can reduce 25% exergy loss or more.

There is growing awareness that global warming is becoming a more significant and challenging environmental issue. Thus, the use of a blend of low-GWP refrigerants with pure CO_2 is promising because of the following advantages: Reducing the high operation pressure of a CO_2 system, improving the system energy efficiency, and alleviating the flammability while maintaining a low GWP.

However, in the previous studies, only a few CO_2 binary mixtures were evaluated without comparison with each other. Thus, in this study the blends of CO_2 with ten low-GWP refrigerants are evaluated, in order to screen the promising alternative mixtures for application to a heat pump water heater.

2. System modeling

2.1 System description and working fluid selection

The water-source heat pump water heater system using the CO_2 binary mixtures with low-GWP refrigerants is shown in Fig. 1. The system consists of a compressor, gas cooler/condenser, expansion valve, and evaporator.

The terms “high GWP” and “low GWP” are comparative in nature. United Nations Environment Programme (2010) proposed an explicit definition of low, moderate, and high GWP for greenhouse gases:

- “Low” if GWP < 300;
- “Moderate” if 300 < GWP < 1000;
- “High” if GWP >1000.

In the field of HVAC&R, R134a is a widely used refrigerant that is considered to be environmentally safe refrigerant and essentially non-toxic. However use of R134a must be significantly reduced according to the provisions of Kyoto protocol (UNEP, 1997), because its GWP is as high as 1370 (Calm and Hourahan, 2011). Although R134a belongs to the high-GWP category, it is still selected in this study in respect of its extensive application. The refrigerants selected as potential candidates are shown in Table 1. As can be seen, most of the fluids are low-GWP refrigerants according to the above classification, except for R32 (moderate GWP) and R134a (high GWP). The physical, safety, and environmental data are described in Table 1, and the refrigerants are sorted by normal boiling point (T_b).

2.2 Assumptions for the model

The analysis was conducted based on the following assumptions:

(1) The system runs under steady working condition.

(2) The pressure drop and heat loss of fluid flowing inside the heat exchangers (gas cooler/condenser

and evaporator) and connecting pipes are ignored.
(3) The refrigerant is at saturated state at the evaporator outlet.
(4) The gas cooler/condenser and evaporator are counter-flow heat exchangers.
(5) The heat transfer fluids of both the gas cooler/condenser and evaporator are water at an ambient pressure of 0.1 MPa.

2.3 Energy and exergy mathematical model

For the specified application of a heat pump, the most important factors are the inlet and outlet temperatures of the heat sink and heat source, also called the external conditions. In this work, the aim is to assess suitable working fluids used for water heater. Thus, the heat pump system in this study is specified based on the rating condition provided in the Chinese standards GB/T 21362-2008 (2008) and GB/T 23137-2008 (2008), which is shown in Table 2.

The status points of the refrigerant are determined from the fixed approach temperature difference at the pinch point in the heat exchangers. The pinch point is defined as the location where the minimum temperature difference between the working fluid and secondary fluid appears in the heat exchanger. The pinch temperature differences at the gas cooler/condenser and evaporator are both set to 5 °C in this study. The mass flow rate of working fluid is set as 1 kg/s for simplicity. The modeling algorithm is shown in Fig. 2. The status points of the cycle are determined by means of iteration, with a 0.01 °C tolerance of the pinch temperature difference in the exchangers and a 1 kPa pressure tolerance. The properties of the mixtures are from REFPROP 9.0 (Lemmon et al., 2010). The energy and exergy analysis are .described as the following equations (Lior and Zhang, 2007):

- For the compressor:

$$W_{Com} = m_r \left(h_2 - h_1\right) / \left(\eta_m \eta_e\right) \tag{1}$$

where η_m and η_e are the mechanical and electrical efficiency, respectively, both assumed to be 0.9.

$$I_{Com} = T_0 m_r \left(s_2 - s_1\right) \tag{2}$$

where I_{Com} is the irreversibility at the compression process, and T_0 is dead state temperature specified as 25 °C (298.15 K)

$$\eta_{Com} = \frac{h_{2_s} - h_1}{h_2 - h_1} \tag{3}$$

where η_{Com} is compressor isentropic efficiency, which is set as 0.8 in this study.

- For the gas cooler/condenser:

$$Q_C = m_r \left(h_2 - h_3\right) \tag{4}$$

$$m_{HW} = m_r \left(h_2 - h_3\right) \Big/ \left(h_{HW,out} - h_{HW,in}\right) \tag{5}$$

$$I_C = T_0 \left[m_r \left(s_3 - s_2\right) - m_{HW} \left(s_{HW,out} - s_{HW,in}\right) \right] \tag{6}$$

where Q_C and I_C are the heat exchange capacity and irreversibility inside the gas cooler/condenser, and m_{HW} is the mass flow rate of hot water.

- For the expansion valve:

$$h_4 = h_3 \tag{7}$$

$$I_{Exp} = T_0 m_r \left(s_4 - s_3\right) \tag{8}$$

where I_{Exp} is irreversibility at the expansion process.

- For the evaporator:

$$Q_E = m_r \left(h_1 - h_4\right) \tag{9}$$

$$E_E = m_r \left[h_4 - h_1 - T_0 \left(s_4 - s_1\right) \right] \tag{10}$$

$$m_{CW} = m_r \left(h_1 - h_4\right) \Big/ \left(h_{CW,in} - h_{CW,out}\right) \tag{11}$$

$$I_E = T_0 \left[m_r \left(s_1 - s_4\right) - m_{CW} \left(s_{CW,out} - s_{CW,in}\right) \right] \tag{12}$$

where Q_E, E_E, and I_E are the heat exchange capacity, exergy, and irreversibility inside the evaporator, and m_{CW} is the mass flow rate of chilled water.

- For the total system:

$$COP = \frac{Q_C}{W_{Com}} \tag{13}$$

$$I_{Tot} = I_{Com} + I_C + I_{Exp} + I_E \tag{14}$$

The exergy efficiency (the second law efficiency) for the overall system (Lior and Zhang, 2007):

$$\eta_{Exe} = 1 - \frac{I_{Tot}}{E_E} \tag{15}$$

3. Results and discussion

3.1 Analysis of energy efficiency

3.1.1 Effect of discharge pressure

The previous studies of Kauf (1999) and Liao et al. (2000) indicated that there exists an optimal high pressure for a transcritical CO_2 cycle. However, those analyses were all performed based on the internal status points (i.e., the working fluid side) without considering the external conditions (i.e., the heat transfer fluid side). In practical applications, the external conditions are more significant. Thus, the heat pump water heater system was analyzed based on the inlet and outlet temperatures of the chilled and cooling water in this study. The COP variations with the high pressure using CO_2 and CO_2/R32 (50/50) are shown in Fig. 3(a) and (b), respectively. As can be seen from the figures, the COP first increases significantly and then decreases gradually as the high pressure increases, and a maximum COP occurs at a certain high pressure. The optimal high pressure for the pure CO_2 system is 9.187 MPa, while that of the CO_2/R32 (50/50) system is 5.638 MPa. Whereas in the studies by Kauf (1999) and Liao et al. (2000) the COP curve had a smooth shape, in this study the curve of COP changes sharply at the optimal high pressure. This is because in the previous analyses (Kauf, 1999; Liao et al., 2000), the gas cooler outlet temperature of the refrigerant side was set as a constant. In this study, the outlet temperature of the gas cooler (T_3) first increases slightly from 8 to 8.4 MPa, then drops suddenly with the increase in gas cooler pressure until 9.2 MPa, to meet the requirements of the constant pinch temperature difference and the water side temperature profile. The outlet temperature then remains at 20 °C with further increase in the pressure, as shown in Fig. 3. As indicated in the study by Liao et al. (2000), the outlet temperature of the gas cooler has a significant influence on the system performance because the heating capacity (Q_h) is very sensitive to its value, and the higher the outlet temperature, the lower the COP becomes. Fig. 3 shows that Q_h increases substantially until the high pressure reaches the optimal value, and turns to a moderate increase. However, the compression work (W) increases linearly, with a low slope. The COP variation tendency of the CO_2/R32 (50/50) system shown in Fig. 3(b) is similar to that with pure CO_2, indicating that an optimal high pressure also exits for the system using a mixture.

The *T*-*s* diagrams of the two working fluids at different high-side pressures are shown in Figs. 4(a) and (b), respectively. As shown in Fig. 4(a), in the case of P_C = 8 MPa, the status of gas cooler outlet (point 3) is to the right side of the critical point with the temperature being as high as 35.6 °C. This implies that the refrigerant is throttled too early, leading to a relatively low heating capacity and high vapor quality at the inlet of the evaporator (point 4). It can also be seen that the pinch point of the gas cooler (PP_C) appears inside the heat exchanger. With an increase in high-side pressure to P_C = 9 MPa, the CO_2 is further cooled inside the gas cooler to a lower outlet temperature. When the high pressure increases to the optimal value of 9.187 MPa, two pinch points appear in the gas cooler, one inside and one at the outlet of the gas cooler. With a further increase of the high pressure to P_C = 10 MPa, there is only one pinch point again, which is at the outlet of the gas cooler. For the mixture CO_2/R32 (50/50), there are also two pinch points at the optimal high pressure of 5.638 MPa during the heat rejection process. However, the heat rejection process for the CO_2/R32 (50/50) system is below the critical point (i.e., a subcritical cycle). Thus, the heat transfer takes place in the condenser rather than the gas cooler for the CO_2/R32 (50/50) system. Consequently, it can be found that the maximum COP of the heat pump water heater system is achieved at the condition where two pinch points appear in the gas cooler/condenser.

However, in the process of evaporation, the pinch point (PP_E) is located at the inlet of the evaporator for pure CO_2, whereas for CO_2/R32 it is situated at the outlet. This difference is attributed to the difference between the internal and external temperature glides. The temperature glide of CO_2 blends with ten low-GWP and moderate-GWP refrigerants at various mass fractions is shown in Fig. 5. The temperature glide of CO_2/R32 (50/50) is 14.5 °C at the bubble point temperature of 10 °C. However, for pure CO_2 the evaporation temperature is constant, leading to zero internal temperature glide. At the rating condition specified in Table 2, the external temperature glide in the evaporator is 5 °C. Consequently, for the evaporation process of pure CO_2 shown in Fig. 4(a), when the internal temperature glide is smaller than the external one, the pinch point is situated on the inlet side of the refrigerant. For the zeotropic mixture of CO_2/R32 (50/50), shown in Fig. 4(b), the situation is reversed, with the pinch point on the outlet side when the internal temperature glide is smaller.

3.1.2 Effect of mixture fraction

Fig. 5 presents the variation of temperature glide with CO_2 mass fraction (X_{CO2}). For each mixture pair, a maximum temperature glide appears at a certain X_{CO2}. As indicated in our previous study (Dai et al., 2014), the maximum temperature glide is dependent on the normal boiling point (T_b). For the pure

refrigerants studied in this work CO_2 has the lowest T_b, as shown in Table 1, and the larger the difference of T_b between the two components of the zeotropic blends, the higher the maximum temperature glide. As indicated in Fig. 5, the blends of CO_2/R41 and CO_2/R32 show relatively low temperature glide, those of CO_2/R1270 and CO_2/R161 are moderate, and the mixture CO_2/R1234ze has the highest glide temperature.

The analysis in Section 3.1.1 explains that there exists a maximum COP and corresponding optimal high pressure for each working fluid (pure or zeotropic fluid). Thus, to reasonably compare the system performance with different mixtures used in a heat pump water heater, the following comparisons are performed under the optimal working condition with maximum COP. Fig. 6 shows the maximum COP of ten kinds of CO_2 blends with various CO_2 mass fractions at the optimal high pressure. It can be seen from Fig. 6 (a) that except for CO_2/R41, the COP of the mixtures show a saddle-shaped change with CO_2 mass fraction. For CO_2/R41, the COP first increases and then decreases, and a maximum COP of 4.65 is found at $X_{CO2} = 0.4$. In addition, the COP of both the CO_2/R41 mixtures and pure R41 are higher than that of pure CO_2 (COP = 4.47). However, for the other mixtures, there exists a minimum COP in the range of $X_{CO2} = 0.5$–0.8, which is lower than that of pure CO_2. In particular, CO_2/R1234ze (60/40) achieves the lowest COP of 3.45, which is 22.8% lower than that of pure CO_2. Although most blends (except CO_2/R41) present a much lower COP than that of pure CO_2, the mixtures CO_2/R32, CO_2/R161, CO_2/RE170, CO_2/R1270, CO_2/R152a, and CO_2/R290 all give promising results. CO_2/R32 has good performance, with the COP ranging from 4.38 to 4.67 for X_{CO2} changes from 0 to 1, which is comparable to the COP of pure CO_2. In particular, for the cases $X_{CO2} = 0.1$ and $X_{CO2} = 0.8$, it operates with the highest COP of 4.67. Other blends (CO_2/R161, CO_2/RE170, CO_2/R1270, CO_2/R152a, and CO_2/R290) perform better than pure CO_2 at $X_{CO2} = 0.1$–0.2 or $X_{CO2} = 0.9$. It can also be seen from Fig. 6(a) that the pure fluids ($X_{CO2} = 0$) all present a lower COP than that of pure CO_2, except for R41.

In Fig. 6(b) the corresponding optimal high pressure (solid line) and critical pressure (dashed line) are depicted. It can be seen that the optimal high pressure of the mixtures and pure fluids are all lower than that of pure CO_2. Furthermore, the high pressure decreases with the reduction of CO_2 mass fraction. Moreover, the higher the normal boiling point of the refrigerant component is, the more the high pressure can decrease. The mixtures with the three lowest high pressures are CO_2/RE170, CO_2/R152a, and CO_2/R1234ze, whereas CO_2/R41 and CO_2/R32 have the highest high pressures.

It can also be found that under the optimal working condition, the systems using the CO_2/R41 mixture are in a transcritical cycle, because the high pressure is above the corresponding critical pressure at any CO_2 mass fraction. However, for other mixtures, at high CO_2 mass concentration ($X_{CO2} = 0.8$) they are transcritical cycles, and are subcritical cycles at lower X_{CO2}.

The change in shape of the COP curves, as depicted in Fig. 6(a), is mainly caused by the temperature matching in the evaporator. The *T*-*s* diagrams using CO_2/R32 at different CO_2 mass fractions under the optimal high pressures are shown in Fig. 7. It can be seen that for CO_2/R32 (80/20), the mixture in the evaporation process (4-1) shows a good thermal match with the chilled water, with the temperature profiles of the two sides parallel to each other. Furthermore, the heat rejection process (2-3) presents a smooth curve, which approximately passes through the critical point. For the case of CO_2/R32 (20/80), although it is a subcritical cycle, the zeotropic mixture condensation process causes a temperature glide in the condenser, which also shows a proper thermal match with the cooling water. In the above two cases ($X_{CO2} = 0.8$ and $X_{CO2} = 0.2$), the temperature profiles of the internal and external fluids are almost parallel with each other. Because the temperatures of the chilled water are fixed, a good temperature match leads to a relatively high mean evaporation temperature, leading to a much higher COP.

However, for the cases of CO_2/R32 (50/50) and pure R32, the temperature match is inferior to the above two cases. In particular, when $X_{CO2} = 0.5$ the internal temperature glide at the evaporation pressure is as high as 13.5 °C, compared with the external temperature glide of 5 °C. Thus, a poor thermal matching is observed in the evaporator. The temperature difference at the inlet of the refrigerant side (11.2 °C) is much larger than that of the outlet (5 °C). Although a good thermal performance is achieved in the heat rejection process, a negative temperature match in the evaporator causes a relatively low evaporation temperature, which reduces the performance of the whole system. Consequently, high energy efficiency can be achieved based on the condition that there are good thermal matches in both the gas cooler/condenser and evaporator.

Except for R41, the COPs of systems using pure fluids are all lower than with pure CO_2, for example the pure R32 shown in Fig. 7. This is because the critical temperatures of these pure fluids are very high, and the heat rejection takes place in the condenser under isothermal conditions during phase change. This leads to a poor thermal match because of the restriction of the pinch point at the dew point under condensation pressure, resulting in a higher condensation temperature. Therefore, relatively low

COPs are achieved for the pure working fluids. However, for pure R41, the critical thermophysical characteristics are close to that of CO_2, and the maximum temperature glide is 1.8 °C (shown in Fig. 5), which results in a better thermal match in the evaporator. Moreover, as shown in Fig. 6(b), the optimal high pressure of R41 is 5.886 MPa, which is 3.3 MPa lower than that of pure CO_2, leading to a smaller expansion loss. Thus, the performance of pure R41 is preferable to that of pure CO_2.

3.1.3 Effect of hot water outlet temperature

If the outlet temperature of water heater is relatively low, then the tank of the water heater may become a breeding ground for Legionella. Thus, it is necessary to increase the supply water temperature to kill the bacteria. However, the regulations for the outlet temperature of a heat pump water heater are not consistent across different countries. As shown in Table 3, it is the lowest for China with an outlet temperature of 55 °C, and is as high as 65 °C in the Japanese standards.

Thus, the system performances with a wide range of hot water outlet temperature are shown in Fig. 8. As can be seen from the figure, the maximum COP decreases as the hot water outlet temperature increases. In addition, for CO_2/R41 the COP values are all higher than those of pure CO_2 with the outlet temperature ranging from 45 to 65 °C. However, for CO_2/R32 when $X_{CO2} = 0$ or $X_{CO2} = 0.5$, the system performance is marginally inferior to that using pure CO_2, but at $X_{CO2} = 0.2$ or $X_{CO2} = 0.8$, the system operates with a rather high COP that is also better than that of CO_2/R41. Although the performance of the CO_2/R41 system is more robust than CO_2/R32 across the whole range of mass concentrations ($X_{CO2} = 0$–1), at some concentration ratios ($X_{CO2} = 0.2$ or $X_{CO2} = 0.8$) CO_2/R32 is superior to CO_2/R41, with higher COP and lower high pressure.

3.1.4 Effect of chilled water inlet temperature

As indicated by the above analysis, the thermal match in the evaporator has a significant influence on the whole system performance. However, this conclusion was achieved on the basis of the rated condition with external temperature glide of 5 °C in the evaporator. In contrast, in practical applications, the external temperature glide varies with the seasonal and climatic conditions. Thus, the following results are achieved from analyses with the chilled water outlet temperature of 10 °C as specified in Table 1, but with the inlet water temperature changing from 12.5 to 30 °C. The results are shown in Fig. 9. For CO_2/R41, the COP is almost constant, due to the low value of temperature glide in the evaporator. For CO_2/R32, the COP of the blends first increases and then remains constant. For the cases of CO_2/R1270 and CO_2/R161, the shapes of the COP curves are similar. In particular, at $X_{CO2} = 0.5$, the COPs increase monotonically with the inlet temperature, and reach maximum values of 5.90 and 6.06, respectively, when the inlet temperature is 30 °C for the two mixtures. This can also be attributed to the temperature match in the evaporator, as shown in Fig. 10.

Fig. 10 illustrates the *T*-*s* diagrams of a CO_2/R161 (80/20) system under different chilled water inlet temperatures ($T_{W, E, in}$). The temperature glide of CO_2/R161 (80/20) is 19.5 °C at the dew point of 10 °C. It can be found that in the case of a chilled water inlet temperature of 15 °C, as shown in Fig. 10(a), the evaporator presents a bad thermal match: At the evaporator inlet on the refrigerant side, the approach temperature difference between the internal and external fluids is extremely high (17.1 °C), leading to a large irreversibility and reducing the mean evaporation temperature. With the increase of the chilled water inlet temperature, as shown in Fig. 10(b), the two temperature profiles gradually become parallel to each other, and the COP also increases, as shown in Fig. 9(d). When the inlet temperature increases to 26.5 °C, as shown in Fig. 10(c), two pinch points appear at both the inlet and outlet of the evaporator. However, with a further increase in inlet temperature ($T_{W, E, in} = 30$ °C), shown in Fig. 10(d), the COP will not change because under this working condition the external temperature glide (20 °C) is larger than the internal one (16.5 °C), and the pinch point shifts to the inlet side of the evaporator on the refrigerant side. Consequently, it can be concluded from the above analysis that a proper temperature match in the evaporator leads to a good system thermal performance. The pure fluids are suitable for a working condition with relatively low external temperature glide, but for high external temperature glide, the zeotropic mixtures are superior for dealing with the temperature change that occurs in the process of phase change.

From the above analysis, it can be found that CO_2/R41 at various concentration ratios is a good choice to substitute for pure CO_2, for use in a heat pump water heater, because of its robust system performance, relatively low GWP, and low rejection pressure. Furthermore, the flammability can be reduced with the addition of CO_2. CO_2/R32 is also a suitable candidate because of its rather high COP and mild temperature glide. Therefore, it is more suitable for use in a heat pump water heater with moderate temperature glide (~10 °C) on the chilled water side. Moreover, the high pressure can also be distinctly reduced. However, the other binary mixtures are not recommended because their temperature glides are extremely large. The internal temperature glide of these binaries can hardly match with the external temperature glide, except at some special concentration ratio with low or moderate temperature glide, such as $X_{CO2} = 0.1$.

3.2 Analysis of exergy efficiency

The exergy efficiency is equivalent to the thermodynamic perfectibility (Ma et al., 2012). Thermodynamic perfectibility is also called Second Law efficiency (Lior and Zhang, 2007), which is defined as the ratio of the system COP to that of the corresponding Carnot cycle (Yuan et al., 2011):

$$\eta_{TP} = \frac{COP}{COP_{Carnot}} \tag{16}$$

The Carnot cycle COP is related to the temperatures of the heat sink and source. In this study, those temperatures are specified in Table 2. Thus, COP_{Carnot} is a constant under the rated working condition, and there also exists a maximum exergy efficiency for each component, which is shown in Fig. 11. It can be seen that the exergy efficiency curves have the same variation tendency as those of the maximum COP shown in Fig. 6(a).

The irreversibility per unit heating capacity (i) can directly represent the performance of the system, and is defined as:

$$i = \frac{I}{Q_C} \tag{17}$$

The values of i for each component are depicted in Fig. 12. The compressor performs the largest irreversibility among the four major components for all of the fluids studied in this paper. For pure CO_2, the irreversible loss in the throttle valve (i_T) is the second largest, because of the huge pressure difference between the high- and low-side pressures, but for pure low-GWP refrigerants, or for the binaries with low X_{CO2}, i_T is the lowest of the four major components of the heat pump system. This is because a lower pressure drop in the throttle process leads to a small irreversibility. It can also be found that the curves of i_C and i_T show an inverse trend with the variation of X_{CO2}. The phenomenon is attributed to the fact that with the decrease in X_{CO2} the pressure difference between high- and low-side pressures reduces, but the thermal match deteriorates due to the system changing from transcritical to subcritical. Thus, the irreversibilities in the two components complement each other. It can also be noted from the figure that the variation tendency of i_{Tot} is the same as that of i_E. Therefore, it can be concluded that the irreversibility occurring in the evaporator is the depending factor to the performance of system. Thus, a proper thermal match in the evaporator dominates the whole heat pump system performance.

4. Conclusions

In this study, carbon dioxide blends with ten low-GWP working fluids were systematically evaluated for use in a heat pump water heater, based on the method of pinch point with the specified temperatures of the heat transfer fluids. The effects that the discharge pressure, component ratio, hot-water outlet temperature, and chilled water inlet temperature had on the thermal performance of the system were analyzed. The following conclusions were drawn from this study:

(1) A maximum COP was obtained at a corresponding optimal high pressure for each component ratio, when two pinch points appear in the gas cooler/condenser. The addition of low-GWP working fluids to pure CO_2 can reduce the high pressure, which decreases as the CO_2 mass fraction decreases.

(2) The system with mixture CO_2/R41 is a transcritical cycle and operates with a high COP. However, for the other binary mixtures, the system changes to a subcritical cycle at lower X_{CO2}. The temperature glide of the mixtures that occurs in the gas cooler/condenser can be well matched to that of the hot water.

(3) The temperature match in the evaporator plays a leading role for the whole system performance. A proper temperature match in the evaporator promoted high COP and reduced the irreversibility.

(4) CO_2 mixtures are recommended on the base of the working condition of chilled water temperature glide:

- CO_2/R41 is recommended because of the robust performance at various X_{CO2} under the condition of low external temperature glide.
- CO_2/R32 is more suitable for its fairly high COP and lower high-side pressure in the case of moderate to high external temperature glide (~10 °C).
- The other binary mixtures are not recommended for use in a heat pump water heater, except at some special concentration ratio with low or moderate temperature glide.

Acknowledgement

This work was supported by the National Natural Science Foundation of China (No. 51176133) and the Tianjin Municipal Science and Technology Commission Foundation (No. 12JCYBJC13800).

References

ANSI/AHRI 470-2006. Performance rating of desuperheater/water heaters. Air-Conditioning, Heating,

and Refrigeration Institute (AHRI), USA, 2006.
ANSI/ASHRAE Standard 34-2010. Designation and Safety Classification of Refrigerants. American Society of Heating (ASHRAE), Refrigerating, and Air-Conditioning Engineers, 2010.
Calm, J., Hourahan, G., 2011. Physical, safety, and environmental data for current and alternative refrigerants. Proceedings of 23rd International Congress of Refrigeration, Prague, Czech Republic, (22 pages).
Chen, C.C., Liaw, H.J., Wang, T.C., Lin, C.Y., 2009. Carbon dioxide dilution effect on flammability limits for hydrocarbons. Journal of Hazardous Materials 163, 795-803.
Dai, B., Li, M., Ma, Y., 2014. Thermodynamic analysis of carbon dioxide blends with low GWP (global warming potential) working fluids-based transcritical Rankine cycles for low-grade heat energy recovery. Energy 64, 942-952.
Di Nicola, G., Giuliani, G., Polonara, F., Stryjek, R., 2005. Blends of carbon dioxide and HFCs as working fluids for the low-temperature circuit in cascade refrigerating systems. International Journal of Refrigeration 28, 130-140.
Di Nicola, G., Polonara, F., Stryjek, R., Arteconi, A., 2011. Performance of cascade cycles working with blends of CO_2 + natural refrigerants. International Journal of Refrigeration 34, 1436-1445.
EN 16147-2011. Heat pumps with electrically driven compressors - Testing and requirements for marking of domestic hot water units. Atlanta, GA, 2011.
GB/T 21362-2008. Heat pump water heater for commercial & industrial and similar application. General Administration of Quality Supervision, Inspection and Quarantine of the People's Republic of China, Standardization Administration of the People's Republic of China, Beijing, China, 2008.
GB/T 23137-2008. Heat pump water heat for household and similar application. General Administration of Quality Supervision, Inspection and Quarantine of the People's Republic of China, Standardization Administration of the People's Republic of China, Beijing, China, 2008.
Hakkaki-Fard, A., Aidoun, Z., Ouzzane, M., 2014. Applying refrigerant mixtures with thermal glide in cold climate air-source heat pumps. Applied Thermal Engineering 62, 714-722.
JIS C9220-2011. Residential heat pump water heaters Japanese Industrial Standards Committee, 2011.
JRA 4060-2009. Industrial heat pump water heaters. The Japan Refrigeration and Air Conditioning Industry Association, 2009.
Kauf, F., 1999. Determination of the optimum high pressure for transcritical CO_2-refrigeration cycles. International Journal of Thermal Sciences 38, 325-330.
Kim, J.H., Cho, J.M., Kim, M.S., 2008. Cooling performance of several CO_2/propane mixtures and glide matching with secondary heat transfer fluid. International Journal of Refrigeration 31, 800-806.
Kim, J.H., Cho, J.M., Lee, I.H., Lee, J.S., Kim, M.S., 2007. Circulation concentration of CO_2/propane mixtures and the effect of their charge on the cooling performance in an air-conditioning system. International Journal of Refrigeration 30, 43-49.
Kim, M.H., Pettersen, J., Bullard, C.W., 2004. Fundamental process and system design issues in CO_2 vapor compression systems. Progress in Energy and Combustion Science 30, 119-174.
Kim, S., Kim, M., 2002. Experiment and simulation on the performance of an autocascade refrigeration system using carbon dioxide as a refrigerant. International Journal of Refrigeration 25, 1093-1101.
Kondo, S., Takizawa, K., Takahashi, A., Tokuhashi, K., 2006. Extended Le Chatelier's formula for carbon dioxide dilution effect on flammability limits. Journal of hazardous materials 138, 1-8.
Lemmon, E., McLinden, M., Huber, M., 2010. NIST Standard Reference Database 23. Reference Fluid Thermodynamic and Transport Properties Database (REFPROP), 9.0 ed. National Institute of Standards and Technology (NIST), Gaithersburg, MD.
Liao, S., Zhao, T., Jakobsen, A., 2000. A correlation of optimal heat rejection pressures in transcritical carbon dioxide cycles. Applied Thermal Engineering 20, 831-841.
Lior, N., Zhang, N., 2007. Energy, exergy, and second law performance criteria. Energy 32(4), 281-296.
Lorentzen, G., 1994. Revival of carbon dioxide as a refrigerant. International Journal of Refrigeration 17, 292-301.
Lorentzen, G., 1995. The use of natural refrigerants: a complete solution to the CFC/HCFC predicament. International Journal of Refrigeration 18, 190-197.
Lorentzen, G., Pettersen, J., 1993. A new, efficient and environmentally benign system for car air-conditioning. International Journal of Refrigeration 16, 4-12.
Ma, Y., Tian, H., Liu, C., Yuan, Q., Zeying, Z., Ling, H., 2012. Analysis on energy efficiency standards and thermodynamic perfectibility for products of refrigeration and heat pump. Science Press, Beijing, China.
McLinden, M.O., Kazakov, A.F., Steven Brown, J., Domanski, P.A., 2014. A thermodynamic analysis of refrigerants: Possibilities and tradeoffs for Low-GWP refrigerants. International Journal of Refrigeration 38, 80-92.

Miyara, A., Onaka, Y., Koyama, S., 2012. Ways of next generation refrigerants and heat pump/refrigeration systems. International Journal of Air-Conditioning and Refrigeration 20, 1130002 (11 pages).
Molina, M.J., Rowland, F.S., 1974. Stratospheric sink for chlorofluoromethanes: chlorine atom-catalysed destruction of ozone. Nature 249, 810-812.
Niu, B., Zhang, Y., 2007. Experimental study of the refrigeration cycle performance for the R744/R290 mixtures. International Journal of Refrigeration 30, 37-42.
Onaka, Y., Miyara, A., Tsubaki, K., 2010. Experimental study on evaporation heat transfer of CO_2/DME mixture refrigerant in a horizontal smooth tube. International Journal of Refrigeration 33, 1277-1291.
Regulation (EU) No 517/2014 of the European Parliament and of the Council on fluorinated greenhouse gases and repealing Regulation (EC) No 842/2006. Available from: http://eur-lex.europa.eu/legal-content/EN/TXT/PDF/?uri=CELEX:32014R0517&from=EN
Sarkar, J., Bhattacharyya, S., 2009. Assessment of blends of CO_2 with butane and isobutane as working fluids for heat pump applications. International Journal of Thermal Sciences 48, 1460-1465.
Sun, F., Ma, Y., 2011. Thermodynamic analysis of transcritical CO_2 refrigeration cycle with an ejector. Applied Thermal Engineering 31(6), 1184-1189.
Tao, Y. B., He, Y. L., Tao, W. Q., 2010. Exergetic analysis of transcritical CO_2 residential air-conditioning system based on experimental data. Applied Energy 87(10), 3065-3072.
United Nations Environment Programme (UNEP), 1987. Montreal protocol on substances that deplete the ozone layer, United Nations, New York, USA.
United Nations Environment Programme (UNEP), 2010. Assessment report of the technology and economic assessment panel: Montreal protocol on substances that deplete the ozone layer, Nairobi, Kenya.
United Nations Framework Convention on Climate Change (UNFCCC), 1997. Kyoto Protocol to the United Nations Framework Convention on Climate Change. Kyoto, Japan.
Yang, J. L., Ma, Y. T., Li, M. X., Guan, H. Q., 2005. Exergy analysis of transcritical carbon dioxide refrigeration cycle with an expander. Energy 30(7), 1162-1175.
Yang, J. L., Ma, Y. T., Liu, S. C., 2007. Performance investigation of transcritical carbon dioxide two-stage compression cycle with expander. Energy 32(3), 237-245.
Yuan, Q., Ma, Y., Liu, C., Dai, B., Yan, Q., 2011. Thermodynamic perfectibility based analysis of energy-efficiency standards for air conditioning products in China. Energy and Buildings 43, 3627-3634.
Zhang, X., Wang, F., Fan, X., Wei, X., Wang, F., 2013. Determination of the optimum heat rejection pressure in transcritical cycles working with R744/R290 mixture. Applied Thermal Engineering 54, 176-184.

Figure captions

Fig. 1. Schematic of heat pump water heater system.

Fig. 2. Flow chart of the modeling.

Fig. 3. Thermal performance of heat pump water heater system, variation with discharge pressure. (a) Pure CO_2. (b) CO_2/R32 (50/50).

Fig. 4. *T-s* diagrams of heat pump water heater system under different discharge pressures. (a) Pure CO_2. (b) CO_2/R32 (50/50).

Fig. 5. Temperature glide for blends of CO_2 with low- and moderate-GWP working fluids at bubble point temperature of 10°C.

Fig. 6. Thermal performance of the heat pump system under optimal working condition using various CO_2 blends. (a) Maximum COP. (b) Optimal high pressure and corresponding critical pressure.

Fig. 7. *T-s* diagrams of heat pump water heater system using CO_2/R32 as refrigerants under optimal working condition at different concentration ratios.

Fig. 8. Variation of maximum COP with hot water outlet temperature. (a) CO_2/R41. (b) CO_2/R32.

Fig. 9. Variation of maximum COP with chilled water inlet temperature. (a) CO_2/R41. (b) CO_2/R32. (c) CO_2/R1270. (d) CO_2/R161.

Fig. 10. *T-s* diagrams of heat pump water heater system using CO_2/R161 (80/20) under optimal working condition at different chilled water inlet temperatures. (a) $T_{W,\,E,\,in}$ = 15 °C, (b) $T_{W,\,E,\,in}$ = 25 °C, (c) $T_{W,\,E,\,in}$ = 26.5 °C, (d) $T_{W,\,E,\,in}$ = 30 °C.

Fig. 11. Maximum exergy efficiency variation with mass fraction of CO_2 for different mixtures.

Fig. 12. Irreversibility per unit heating capacity of every component of the system under the condition of maximum exergy efficiency. (a) CO_2/R41. (b) CO_2/R32. (c) CO_2/R1270. (d) CO_2/R290.

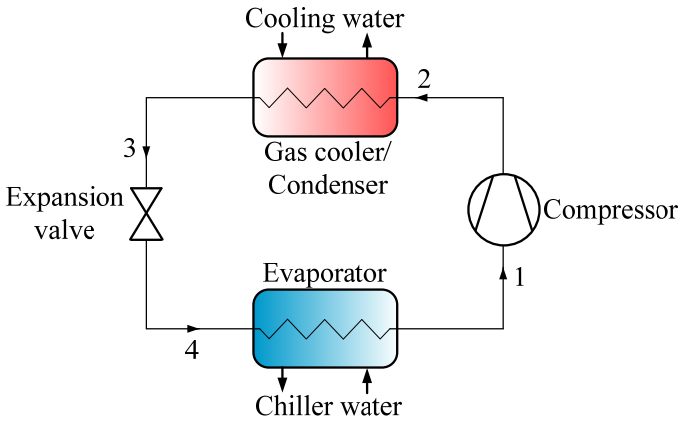

Fig. 1. Schematic of heat pump water heater system.

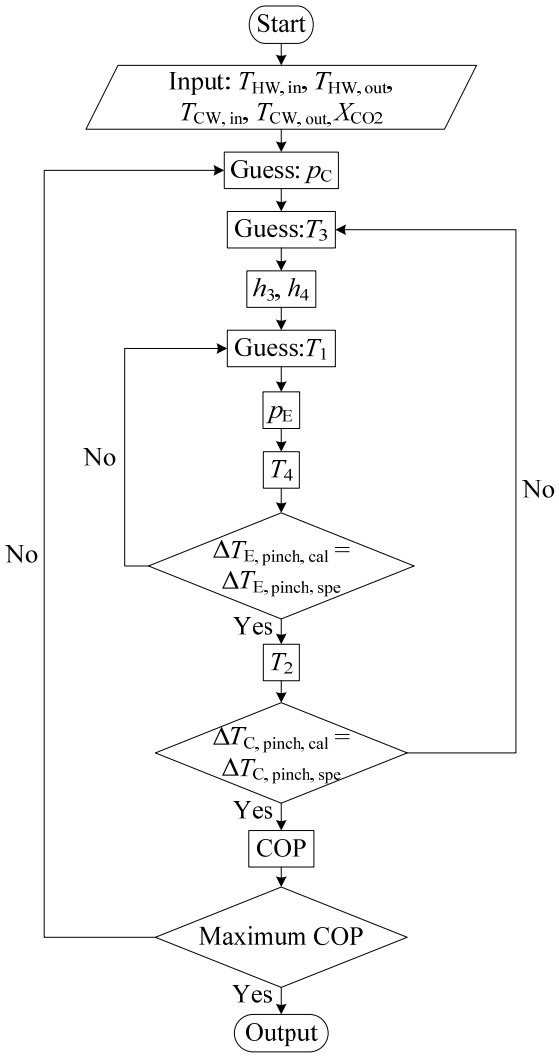

Fig. 2. Flow chart of the modeling.

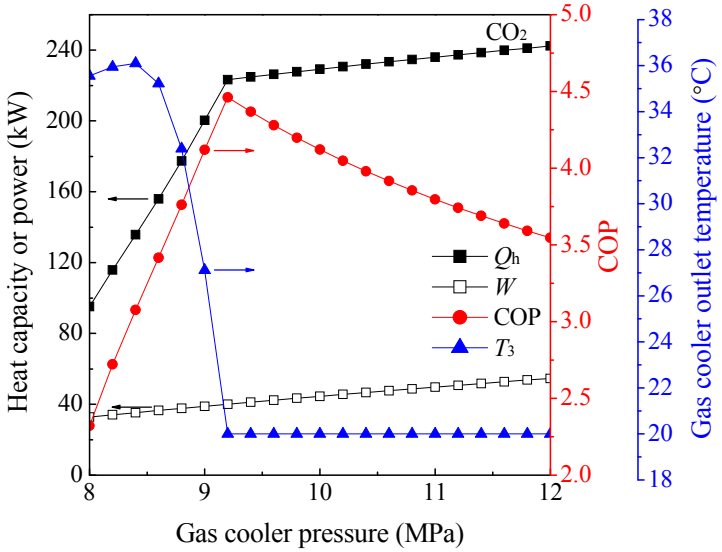

(a)

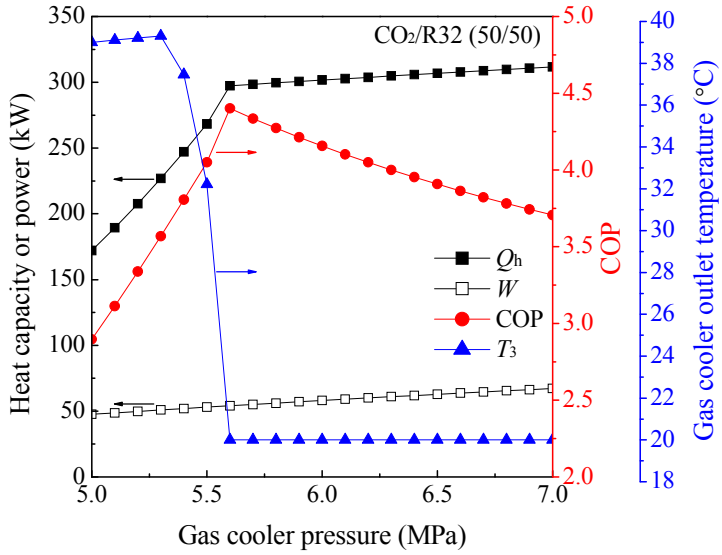

(b)

Fig. 3. Thermal performance of heat pump water heater system, variation with discharge pressure. (a) Pure CO_2. (b) CO_2/R32 (50/50).

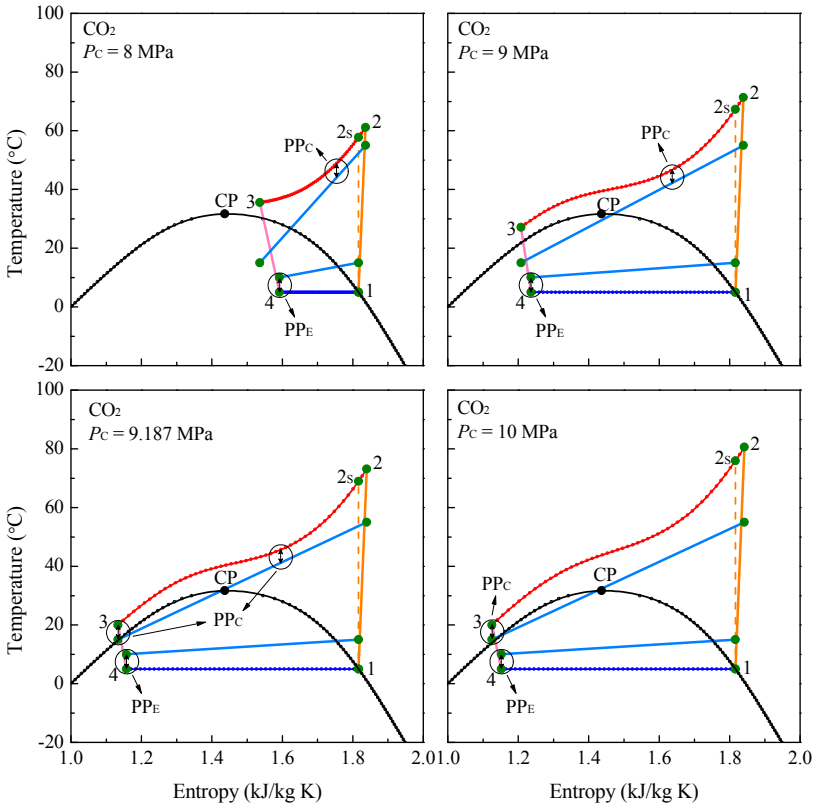

(a)

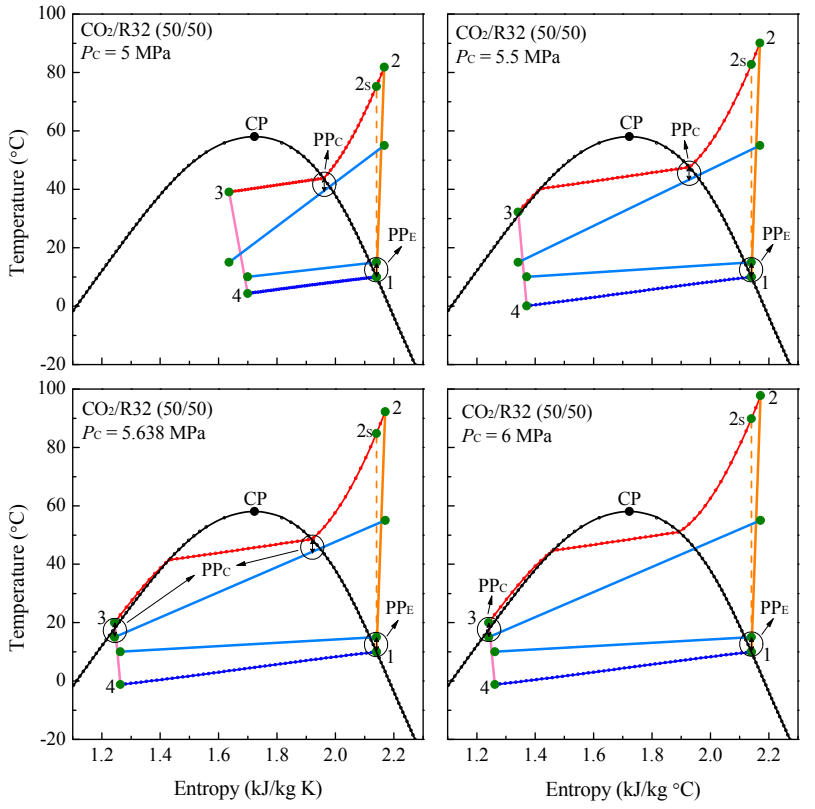

(b)

Fig. 4. *T-s* diagrams of heat pump water heater system under different discharge pressures. (a) Pure CO_2. (b) CO_2/R32 (50/50).

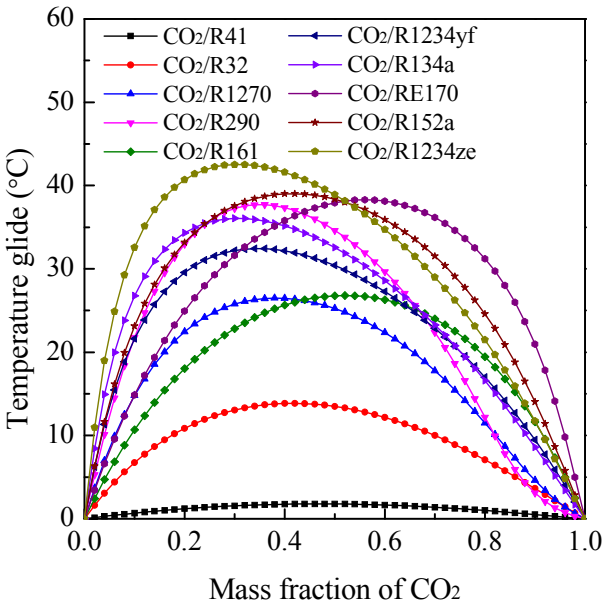

Fig. 5. Temperature glide for blends of CO_2 with low- and moderate-GWP working fluids at bubble point temperature of 10°C.

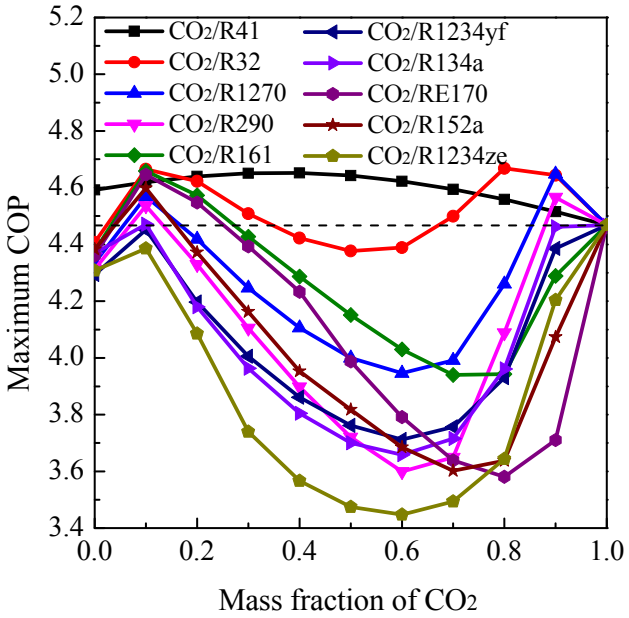

(a)

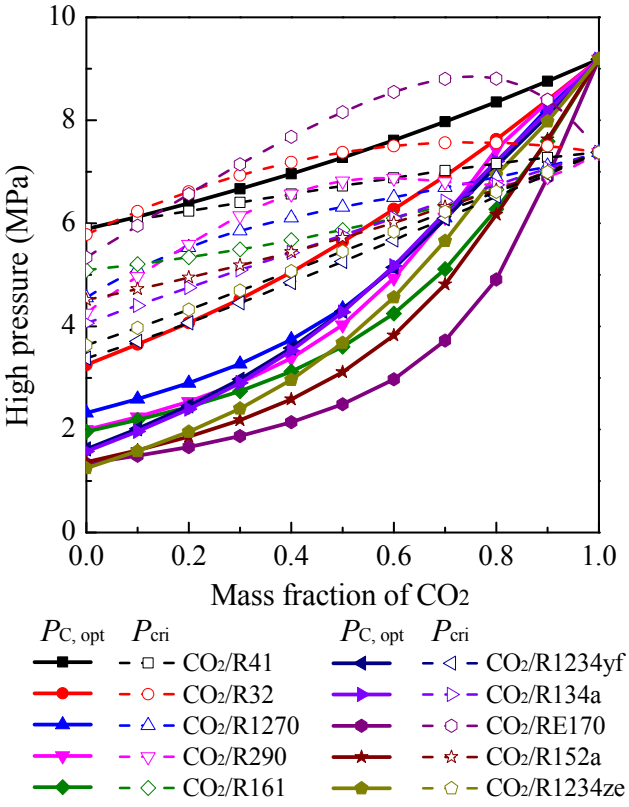

(b)

Fig. 6. Thermal performance of heat pump system under optimal working condition using various CO_2 blends. (a) Maximum COP. (b) Optimal high pressure and corresponding critical pressure.

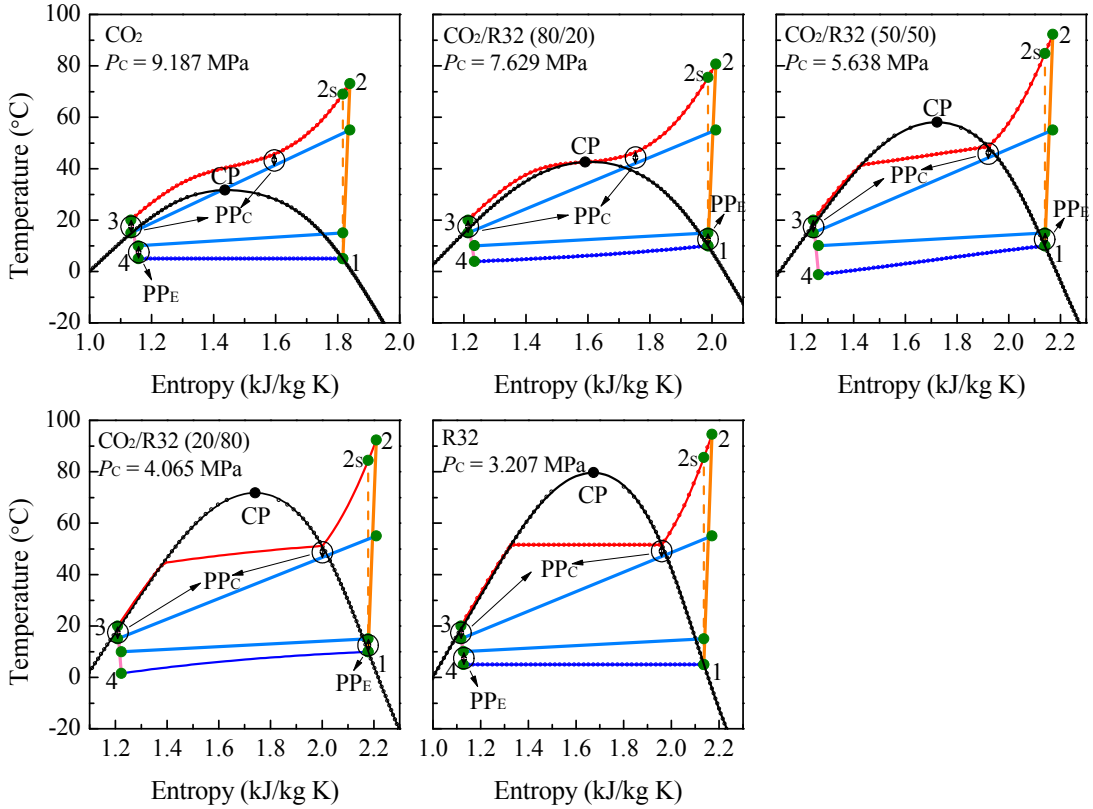

Fig. 7. *T-s* diagrams of heat pump water heater system using CO_2/R32 as refrigerants under optimal working condition at different concentration ratios.

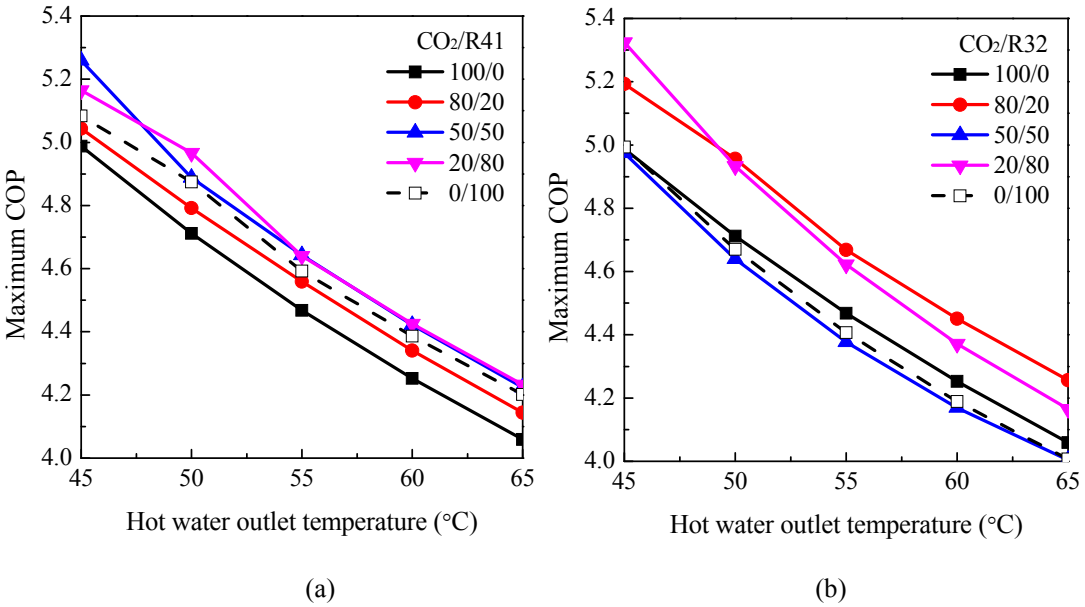

(a) (b)

Fig. 8. Variation of maximum COP with hot water outlet temperature. (a) CO_2/R41. (b) CO_2/R32.

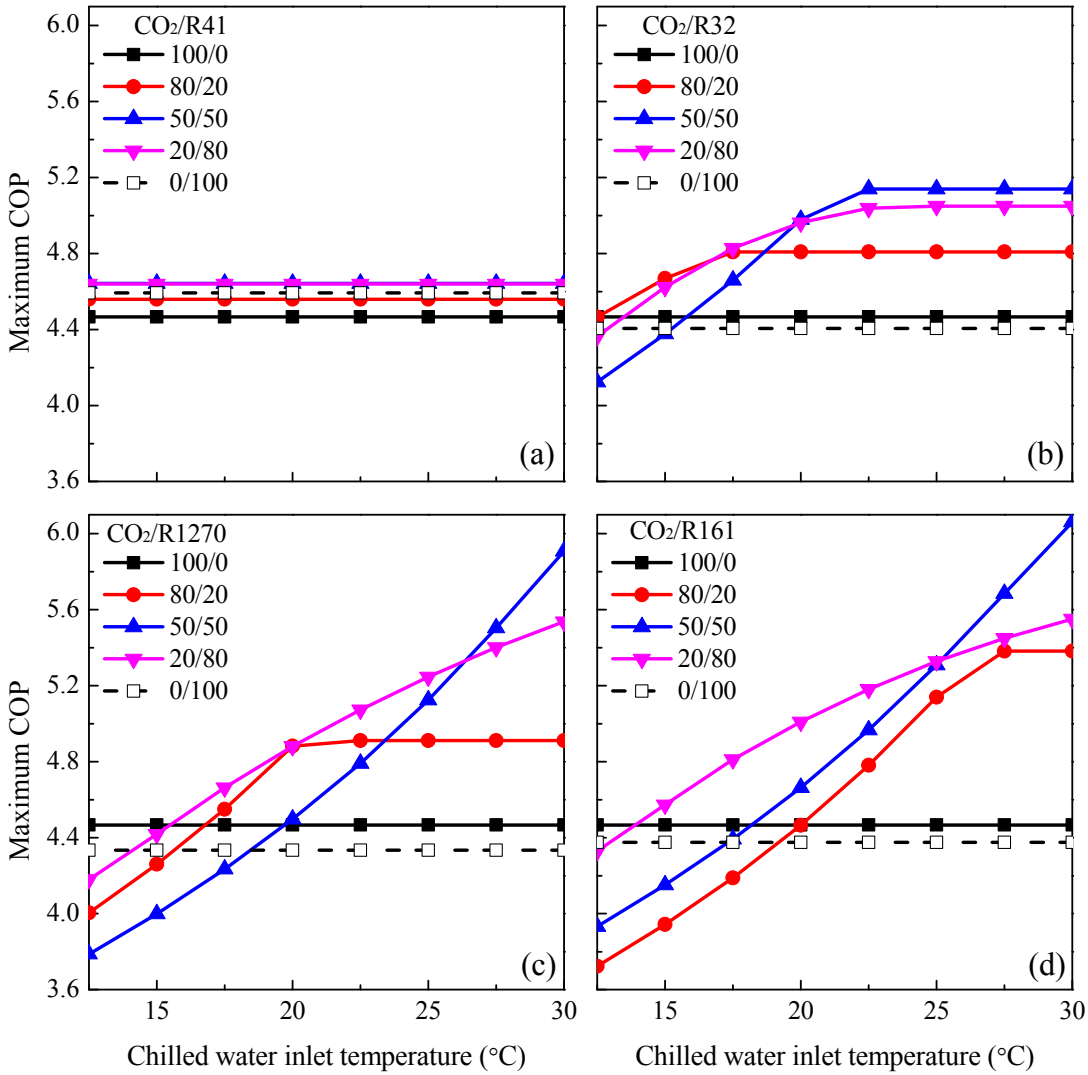

Fig. 9. Variation of maximum COP with chilled water inlet temperature. (a) CO_2/R41. (b) CO_2/R32. (c) CO_2/R1270. (d) CO_2/R161.

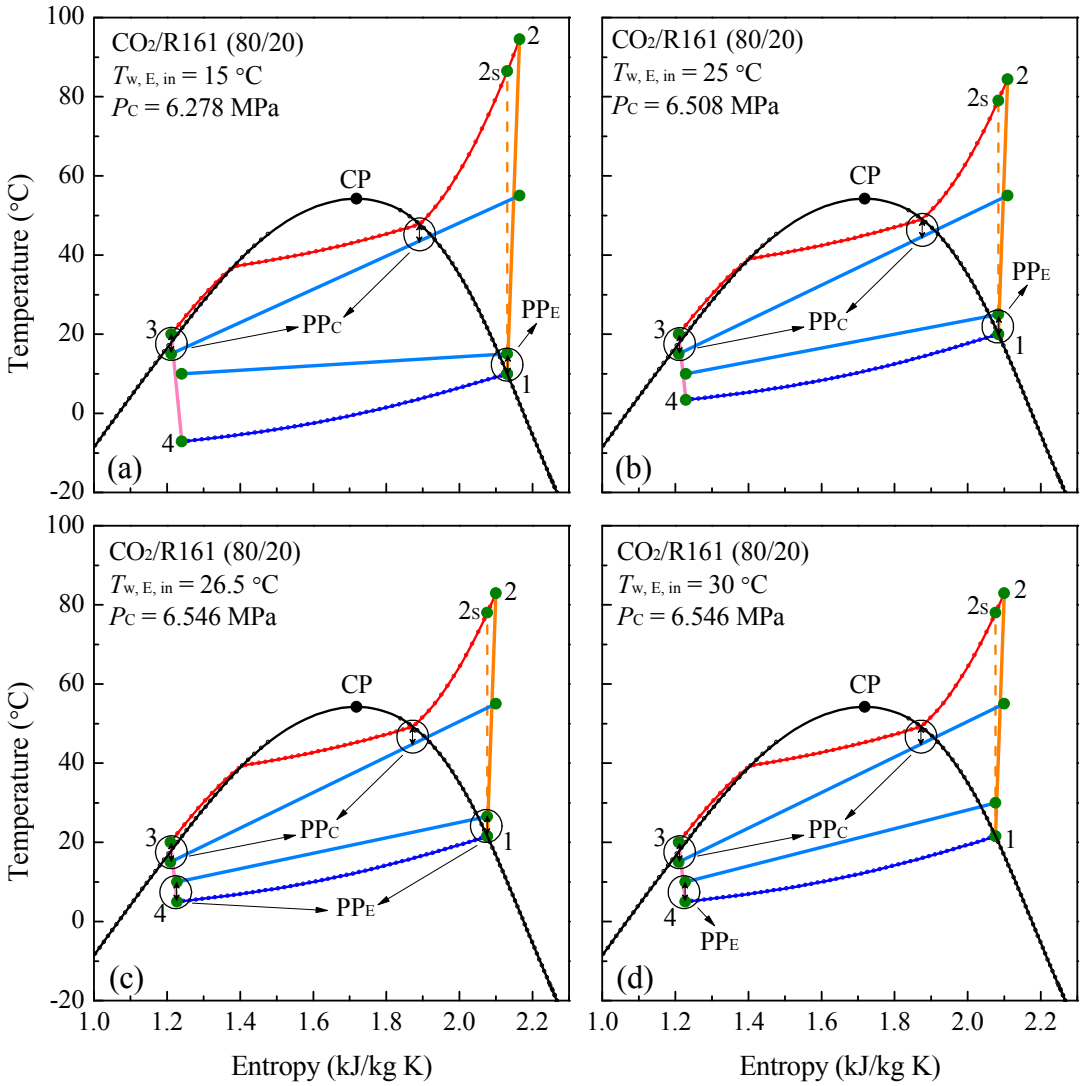

Fig. 10. *T-s* diagrams of heat pump water heater system using CO_2/R161 (80/20) under optimal working condition at different chilled water inlet temperatures. (a) $T_{W,\,E,\,in}$ = 15 °C, (b) $T_{W,\,E,\,in}$ = 25 °C, (c) $T_{W,\,E,\,in}$ = 26.5 °C, (d) $T_{W,\,E,\,in}$ = 30 °C.

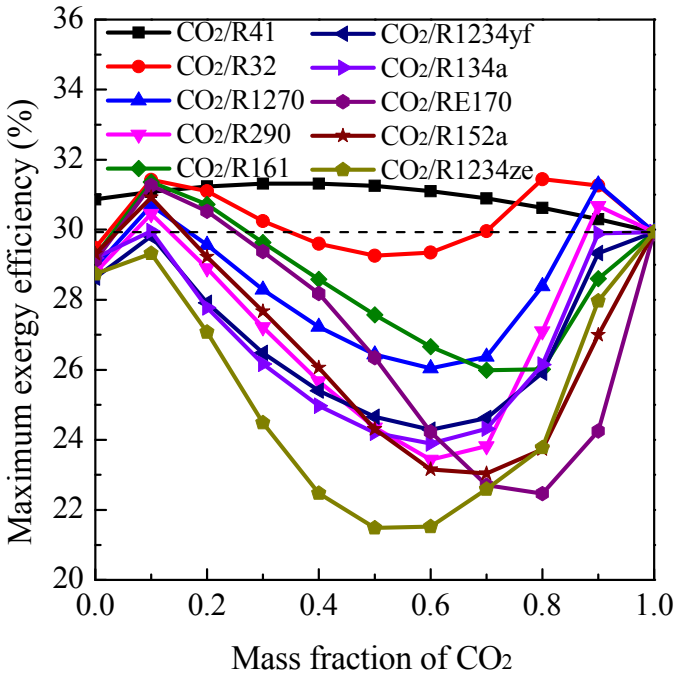

Fig. 11. Maximum exergy efficiency variation with mass fraction of CO_2 for different mixtures.

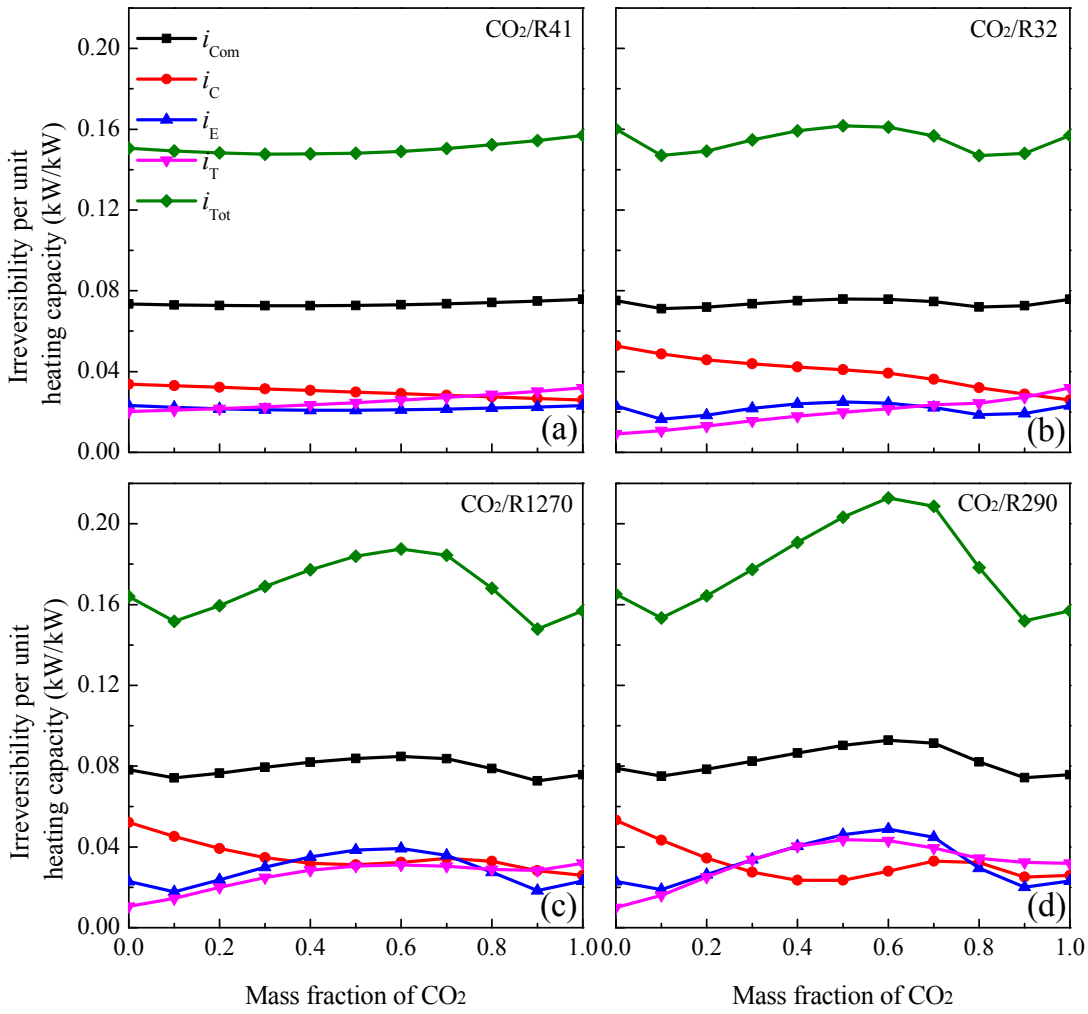

Fig. 12. Irreversibility per unit heating capacity of every component of the system under the condition of maximum exergy efficiency. (a) CO_2/R41. (b) CO_2/R32. (c) CO_2/R1270. (d) CO_2/R290.

Table 1. Physical, safety, and environmental data for refrigerants (Calm and Hourahan, 2011).

Substance	Physical data				Safety data			Environmental data		
	Molecular mass	T_b (°C)	T_{cri} (°C)	P_{cri} (MPa)	OEL (PPMv)	LEL (%)	ASHRAE 34 safety group	Atmospheric life (yr)	ODP	GWP
R744	44.01	−78.4	31.1	7.38	5000	None	A1	>50	0	1
R41	34.03	−78.3	44.1	5.9	-	-	A2	2.8	0	107
R32	52.02	−51.7	78.1	5.78	1000	14.1	A2	4.9	0	675
R1270	42.08	−47.7	92.4	4.66	660	2.0	A3	0.001	0	~20
R290	44.10	−42.1	96.7	4.25	1000	2.1	A3	0.041	0	~20
R161	48.06	−37.6	102.2	5.09	-	3.8	-	0.21	0	12
R1234yf	114.04	−29.5	94.7	3.38	500	6.2	A2L	0.029	0	<4.4
R134a	102.03	−26.1	101.1	4.06	1000	none	A1	14.0	0	1370
RE170	46.07	−24.8	127.2	5.34	1000	3.4	A3	0.015	0	1
R152a	66.05	−24.0	113.3	4.52	1000	4.8	A2	1.4	0	124
R1234ze	114.04	−19.0	109.4	3.64	1000	7.6	A2L	0.045	0	6

Table 2. Standard rating condition of water source heat pump water heater (GB/T 21362-2008; GB/T 23137-2008).

Hot water at gas cooler/condenser side		Chilled water at evaporator side	
Inlet temperature (°C)	Outlet temperature (°C)	Inlet temperature (°C)	Outlet temperature (°C)
15	55	15	10

Table 3. Standards of heat pump water heater of different countries.

Standard	Country	Application field	Specified outlet temperature of hot water (°C)
GB/T 23137-2008	China	Residential	55
GB/T 21362-2008	China	Commercial and Industrial	55
ANSI/AHRI 470-2006	United States of America	-	60
EN 16147-2011	European Union	Residential	60[a]
JRA 4060-2009	Japan	Residential	65
JIS C 9220 -2011	Japan	Industrial	65

a. Equivalent hot water temperature.